

Development of Experimental Techniques for Thermoelectric Properties Characterization of Low-Dimensional Structures

Claudiu L. Hapenciuc¹, Fazeel J. Khan¹, Theodorian Borca-Tasciuc^{1,*} and Gwo-Ching Wang²

¹Mechanical and Aerospace Engineering Department, Rensselaer Polytechnic Institute

²Department of Physics, Rensselaer Polytechnic Institute

Troy, NY 12180, U.S.A.

ABSTRACT

This work reports current efforts in developing experimental techniques applicable for thermoelectric properties characterization at micro and nanoscale. A one-dimensional transport model was used to assess the effects of heat leakage, non-symmetric boundary conditions, and electrical contact resistance, on thermoelectric properties measurements performed by transient Harman method. If the above effects are important, the thermoelectric figure of merit cannot be extracted directly from the ratio between the Seebeck voltage and the resistive voltage drop across the sample. On the other hand, measurements of both thermal conductivity and Seebeck coefficient can be performed if the temperature drop across the sample is acquired simultaneously with the voltage drop. The theoretical model and the experimental technique are validated by measurements performed on bulk calibration samples. Furthermore, this work shows that the spatial resolution of thermoelectric properties characterization methods can be enhanced by using scanning probe based techniques. Preliminary results are presented for Seebeck coefficient measurements of p-type or n-type calibration samples performed using an AFM probe instrumented with a temperature sensor.

INTRODUCTION

Low-dimensional structures may demonstrate a large enhancement of the thermoelectric figure of merit [1], hence measurements of their thermoelectric properties is of high interest. Harman method [2] may provide a fast and reliable way to screen large numbers of samples for high thermoelectric figure of merit ZT. However, implementation of the Harman method for thermoelectric properties characterization of low-dimensional systems must consider several issues: (1) enhanced spatial and temporal resolution is needed as dimensions of the samples may range from a few microns (e.g. across the thickness of a thermoelectric film), to a few nanometers (the diameter of a nanowire); (2) nanostructures may be subjected to significant heat losses during the measurement (e.g. heat sinking effect for film-on-substrate systems, and also due to relatively large size of the electrodes); (3) electrical and thermal contact resistance between the sample and electrodes may become important.

This work investigates the effect of heat leakage, non-symmetric boundary conditions, and electrical contact resistance on the Harman based characterization. Moreover, it reports preliminary results on the implementation of scanning probe techniques for thermoelectric properties measurements. A theoretical model was developed and validated by measurements

* Corresponding author. Electronic address: borcat@rpi.edu.

performed on bulk calibration samples. It was found that when heat leakage and contact resistance effects are important, the thermoelectric figure of merit cannot be extracted directly from the ratio between the Seebeck voltage and the resistive voltage drops across the sample. On the other hand, measurements of both thermal conductivity and Seebeck coefficient are possible if the temperature drop across the sample is acquired simultaneously with the voltage drop. Furthermore, this work shows that the spatial resolution of thermoelectric properties characterization methods can be enhanced by using scanning probe based techniques. Preliminary results are presented for Seebeck coefficient measurements of p-type or n-type calibration samples performed using an AFM probe instrumented with a resistive temperature sensor.

THEORETICAL MODEL

The classical set-up of the transient Harman method is shown in Fig. 1 (a). When DC current is passed through the free standing specimen, Peltier effects at the junctions between the sample and the current electrodes give rise to a temperature drop across the specimen, which in turn generates a Seebeck voltage drop. Assuming the electrodes have negligible electrical contact resistance with the sample and insignificant heat leakage effects, the non-dimensional figure of merit is determined straightforward from the ratio between the Seebeck voltage drop (V_S) and the resistive voltage drop (V_p) across the sample. The Seebeck voltage is the voltage measured immediately after the current is switched off in the circuit, while the resistive voltage drop is the difference between the total voltage drop and the Seebeck voltage. A nanoscale implementation of the transient Harman method is shown in Fig. 1(b). An electrically conductive AFM tip is used as one electrode while the second electrode is an electrically conductive film sandwiched between the substrate and the nanostructure. The spatial resolution of scanning probe microscopes scanners may allow positioning of the tip on the top surface of a single nanowire. However, heat leakage through the AFM probe and substrate, thermal and electrical contact resistance, and non-symmetrical boundary conditions may affect the measurement of the thermoelectric properties. To assess the influence of the above parameters a one-dimensional steady state model was developed for the electrical and thermal transport in a simplified

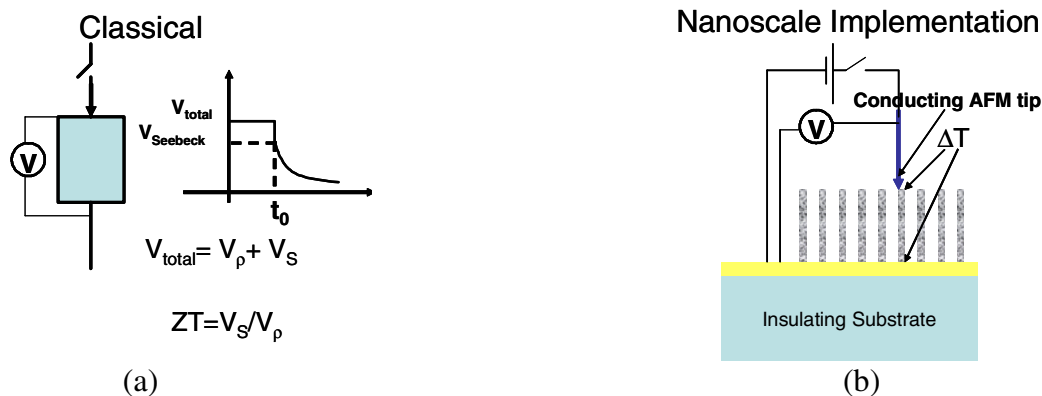


Figure 1. The transient Harman method: (a) the classical experimental setup and, (b) implementation for thermoelectric properties characterization of nanostructures.

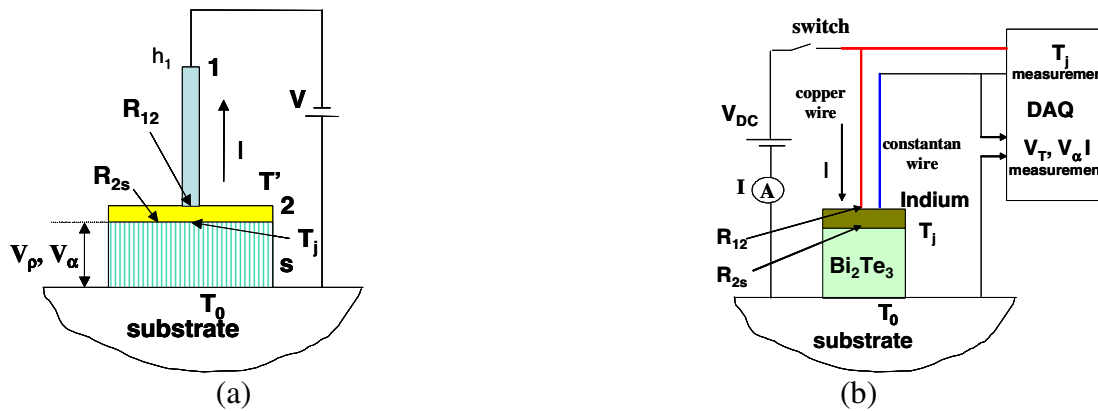


Figure 2. a) Theoretical model; and b) Experimental setup for model validation.

configuration of the system as shown in Fig.2 (a).

The top electrode (1) comes in contact with the sample surface which is covered by a metallic electrode (2). Heat transfer coefficient h_1 is assumed for electrode 1 and an electrical contact resistance R_{12} is assigned between (1) and (2). The electrical contact resistance between the specimen (S) and (2) is R_{2s} . The temperature at the specimen-substrate interface is assumed to remain constant under operation and equal to the ambient temperature T_0 . No thermal boundary resistance effects are currently included. A voltage V is applied to the system and the temperature rise on the top surface (T') and the Seebeck and resistive voltage drops across the sample are determined as a function of the thermal and thermoelectric properties of the system. If the above voltages are measured experimentally, the model may be used to fit for the thermoelectric properties of the sample. However, since the resistive voltage drop across the specimen is the sum of the voltage drop across R_{2s} and sample resistance, one of these two resistances must be known in order to be able to determine the thermal conductivity of the specimen. The electrical contact resistance and the resistance of the specimen can be inferred from measurements performed on similar samples with different thickness. A more detailed discussion on the model will be given elsewhere [3]. In this work the theoretical model is validated by performing an experiment with a calibration sample as described below.

EXPERIMENTAL VALIDATION

The experimental setup employed for validation of the theoretical model is shown in Fig. 2 (b). An n-type Bi_2Te_3 element from a commercially available thermoelectric device serves as the test specimen. The thermoelectric device was broken such that one side of the element is still in contact with the original electrode deposited on the ceramic substrate while the top surface of the specimen is free. A fine copper wire is brought in mechanical contact with the surface and used to pass electrical current through the specimen. A constantan wire is used to measure the voltage drop across the sample. Moreover, the pair of copper-constantan wires is employed as a thermocouple (immediately after the current is switched off) in order to measure the steady state temperature on the top surface of the sample. Figure 3 shows an example of the time dependent voltage (Fig. 3(a)) and temperature signals (Fig. 3b) collected by the computer controlled data acquisition system. The experiment is performed for direct and reverse directions of the current passing through the specimen, therefore both heating (h) and cooling (c) of the top surface of the

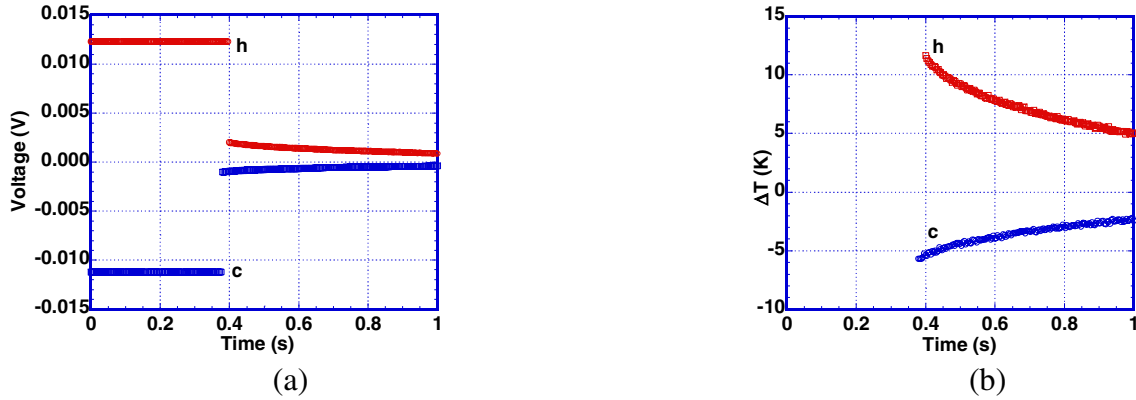


Figure 3. Experimental signals collected in heating (h) and cooling (c) of the top surface of the specimen: a) the voltage drop and b) the temperature drop across the sample.

sample is observed. Moreover, the experiment is repeated for different values of the current and the experimentally measured current, Seebeck voltage (V_S) and temperature drop (ΔT) across the sample, are shown in Table I. The determination of the Seebeck coefficient (α), is straightforward. The experimental values are in very good agreement with the ($-211\mu\text{V}/\text{K}$) value provided by the manufacturer. Also shown in the table are the estimated resistive voltage drops across the sample calculated based on the manufacturer data for the electrical resistivity. This allows for the determination of the electrical contact resistance R_{2s} . The thermal conductivity of the sample is then determined by fitting the experimental temperature rise with predictions of the transport model developed in the previous section. Since the only unknowns are the electrical contact resistance (R_{12}), and thermal conductivity, both parameters can be determined by fitting simultaneously the heating and cooling temperature rise data. The examples used in the table consider different heating and cooling data pairs (2 with 3 and 3 with 4). The determined thermal conductivity ranges between 1.35-1.39W/mK, which is in relatively good agreement with the manufacturer value of 1.5W/mK. Also in very good agreement is the determined value of ZT (0.86 compared with 0.85). It should be noted that the value of ZT is significantly larger than the ratio V_S/V_p obtained under the current experimental conditions. This result emphasizes the

Table I Experimental signals and fitted thermoelectric properties data.

Trial	$V_S(\mu\text{V})$	$\Delta T(^{\circ}\text{C})$	$\alpha(\mu\text{V}/^{\circ}\text{C})$
1	510	2.98(c)	-206.1
2	2000	11.52(h)	-208.46
3	1010	5.72(c)	-211.6
4	2200	12.63(h)	-209.18
Trial	$V_p(\mu\text{V})$	$I(\text{A})$	$R_{2s}(\Omega)$
1	7570	0.116	0.0467
2	10280	0.158	0.0465
3	10220	0.159	0.0457
4	10568	0.163	0.0462
Data fitted	ZT	$K(\text{W}/\text{mk})$	$R_{12}(\Omega)$
2 with 3	0.86	1.35 1.39	0.03
3 with 4	0.86	1.36 1.39	0.06

effectiveness of the developed model to extract the intrinsic thermoelectric properties of the specimen when heat leakage and contact resistance effects are significant.

SPM BASED MEASUREMENTS

Performing thermoelectric properties characterization of low-dimensional systems such as individual nanowires requires employment of techniques capable of high spatial resolution. Scanning probe techniques are among the most suitable for nanoscale characterization due to their unsurpassed spatial resolution. Current state of the art methods for temperature mapping at nanoscale include AFM/STM modified probes with built-in temperature sensors [4, 5, 6] and near-field scanning optical thermometry using tapered optical fiber [7] or solid immersion lens [8]. This section reports preliminary Seebeck coefficient measurements performed with an AFM probe instrumented with a resistive temperature sensor.

The principle of the method is shown in Fig. 4 (a) while Fig. 4(b) shows a schematic of the resistive probe. The commercially available thermal probe is made from a Wollaston wire shaped as a tip and etched to uncover the Pt-Rh core. The Pt-Rh core is $5\mu\text{m}$ in diameter. The probe is mounted on an Autoprobe CP Park Scientific AFM. A Wheatstone bridge is used to measure the average temperature rise of the probe. The bridge is initially balanced at low AC excitation voltages. Higher AC excitation voltages of the Wheatstone bridge are used to create a DC temperature rise in the probe above ambient temperature. The heated probe is brought in contact with the sample surface. The DC temperature rise of the probe generates a DC Seebeck voltage drop across the sample, which is measured by a DC voltmeter. The experimental Seebeck voltage as a function of the maximum temperature rise of the tip (extracted from a one-dimensional heat conduction model along the heated probe) is shown in Fig. 5, respectively for n-type (Fig. 5(a)) and p-type (Fig. 5(b)) Bi_2Te_3 calibration samples. The Seebeck voltage has a linear dependence on the temperature drop and the slope of the line fit is used to extract the Seebeck coefficient. The measured Seebeck coefficient for the p-type sample is quite close to the manufacturer value, however the result for the n-type sample is $\sim 25\%$ lower. The reasons for the

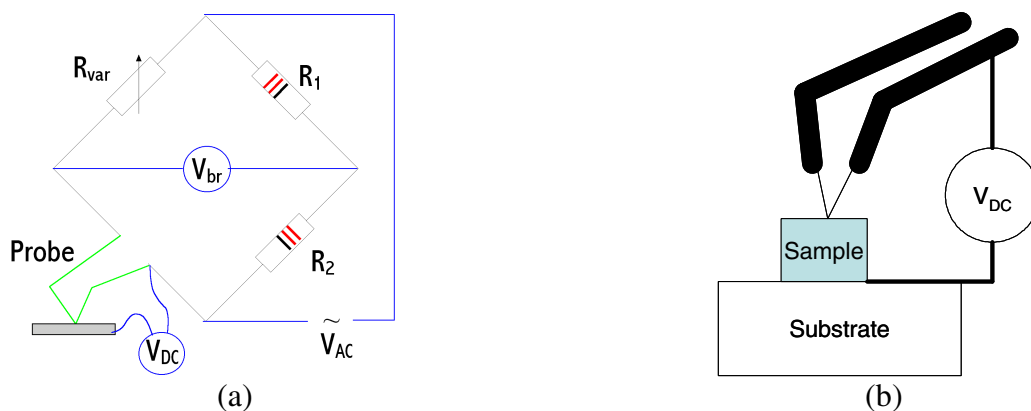


Figure 4. Seebeck coefficient measurement using a resistive AFM thermal probe: a) heating and temperature measurement setup, and b) schematic of the probe configuration.

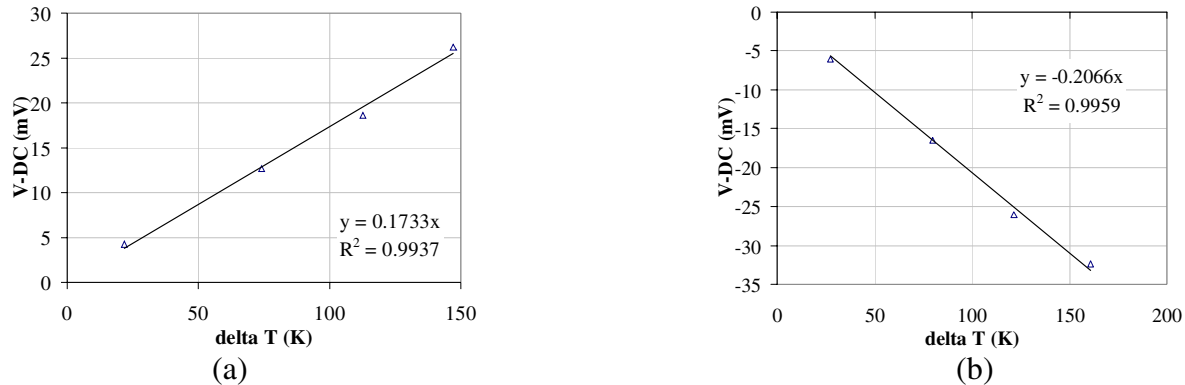


Figure 5. Measured Seebeck voltage as a function of temperature drop across the sample thickness for a) n-type, and b) p-type, Bi₂Te₃ calibration samples.

observed discrepancy is currently under investigation. The experiments need to be repeated under lower temperature difference conditions and the effects of thermal boundary resistance must be assessed.

CONCLUSIONS

A one-dimensional transport model was used to assess the effects of heat leakage, non-symmetric boundary conditions, and electrical contact resistance, on the thermoelectric properties measurements performed by the transient Harman method. Measurements of both thermal conductivity and Seebeck coefficient can be performed if the temperature drop across the sample is acquired simultaneously with the voltage drop. The theoretical model and the experimental technique are validated by measurements on bulk calibration samples. Preliminary results are presented for Seebeck coefficient of p-type or n-type calibration samples performed using an AFM probe instrumented with a resistive temperature sensor.

ACKNOWLEDGMENTS

The authors acknowledge funding support from NSF under MCE grant 0210587.

REFERENCES

1. G. Chen, M.S. Dresselhaus, G. Dresselhaus, J.-P. Fleurial, and T. Caillat, *Int. Mater. Rev.*, **48**, 45 (2003).
2. T. C. Harman, J. H. Cahn, and M. J. Logan, *J. Appl. Phys.*, **30**, 1351 (1959).
3. C. L. Hapenciuc and T. Borca-Tasciuc, "Harman based measurement of thermoelectric properties of nanostructures," manuscript in preparation.
4. L. Shi and A. Majumdar, *J. Heat. Transf.*, **124**, 329 (2002).
5. C. C. Williams and H. K. Wickramasinghe, *Appl. Phys. Lett.*, **49**, 1587 (1986).
6. S. Lefèvre, S. Volz, J.-B. Saulnier, C. Fuentes, and N. Trannoy, *Rev. Sci. Instrum.*, **74**, 2418 (2003).
7. K. E. Goodson and M. Asheghi, *Microscale Thermophysical Engineering*, **1**, 225 (1997)..
8. D. A. Fletcher, K. B. Crozier, C. F. Quate, G. S. Kino, K. E. Goodson, D. Simanovski, and D. V. Palanker, *Appl. Phys. Lett.* **77**, 2109 (2000).